Talanta 84 (2011) 1124–1132

Contents lists available at ScienceDirect

Talanta

journal homepage: www.elsevier.com/locate/talanta

Synthesis of surface molecularly imprinted polymer and the selective solid phase extraction of imidazole from its structural analogs

Guifen Zhu[a], Jing Fan[a,*], Yanbu Gao[a], Xia Gao[a,b], Jianji Wang[a,*]

[a] School of Chemistry and Environmental Science, Henan Key Laboratory for Environmental Pollution Control, Key Laboratory for Yellow River and Huai River Water Environmental and Pollution Control, Ministry of Education, Henan Normal University, Xinxiang, Henan 453007, PR China
[b] Department of Public Health, Xinxiang Medical University, Xinxiang, Henan 453003, PR China

ARTICLE INFO

Article history:
Received 5 November 2010
Received in revised form 1 March 2011
Accepted 8 March 2011
Available online 16 March 2011

Keywords:
Imidazole
Molecularly imprinted polymer
Synthesis
Solid phase extraction

ABSTRACT

A surface molecularly imprinted polymer (MIP) was synthesized by using imidazole as the template and modified silica particles as the support material. The static adsorption, solid phase extraction (SPE) and high-performance liquid chromatography (HPLC) experiments were performed to investigate the adsorption properties and selective recognition characteristics of the polymer for imidazole and its structural analogs. It was shown that the maximum binding capacities of imidazole on the MIP and the non-imprinted polymer (NIP) were 312 and 169 $\mu mol\ g^{-1}$, respectively. The adsorption was fast and the adsorption equilibrium was achieved in 30 min. The binding process could be described by pseudo-second order kinetics. Compared with the corresponding non-imprinted polymer, the molecularly imprinted polymer exhibited much higher adsorption performance and selectivity for imidazole. The selective separation of imidazole from a mixture of 1-hexyl-3-methylimidazolium bromide ([C_6mim][Br]) and 2,4-dichlorophenol could be achieved on the MIP–SPE column. The recoveries of imidazole and [C_6mim][Br] were 97.6–102.7% and 12.2–17.3%, respectively, but 2,4-dichlorophenol could not be retained on the column. The surface molecularly imprinted polymer presented here may find useful application as a solid phase absorbent to separate trace imidazole in environmental water samples. This may also form the basis for our research program on the preparation and application of alkyl-imidazolium imprinted polymers.

1. Introduction

In recent years, people are increasingly interested in using ionic liquids, especially alkyl-imidazolium based ionic liquids, for chemical synthesis, biocatalytic transformation, electrochemical device design and analytical and separation process, mainly due to their "green" characteristics [1,2]. Ionic liquids have negligible vapor pressure and are rarely flammable or explosive, suggesting that they present no air pollution or environmental risk in closed processes. However, it has been shown that alkyl-imidazolium based ionic liquids are toxic to mammalian zooblast [3,4], microorganism [5,6] and among others. The ionic liquids are just as toxic as conventional organic solvents, and sometimes two-to-four orders of magnitude more toxic than the organic solvents [7]. The toxic is mainly ascribed to the alkyl-imidazolium cations. Therefore, the wide application of ionic liquids would inevitably result in the loss of the ionic liquids into water ecosystems, leading to pollution of water, soil and ecological environment. Accordingly, it is important to assay trace alkyl-imidazolium based ionic liquids in environmental samples.

In traditional analysis methods of organic compounds, HPLC [8], spectroscopy [9] and ion chromatogram [10] etc., are useful for the systems with little interfere and high target concentration. However, imidazole ring of cations of the ionic liquids is UV active, and many organics have similar absorbance profiles in the UV–visible range with imidazole ring. Thus the signal overlapping is a serious problem for the direct determination of alkyl-imidazolium based ionic liquids [11]. Due to this characteristic of ionic liquids and complex of the environmental samples, it is difficult to assay the target compounds directly by using traditional analysis methods. Consequently, the establishment of effective methods to separate and assay alkyl-imidazolium based ionic liquids in complex matrixes is very important.

Molecularly imprinting of synthetic polymer is an approach in which functional monomer and cross linker are copolymerized in the presence of template molecule. Removal of the template molecule from the obtained polymer by simple solvent extraction reveals the complementary binding sites that can recognize the template molecule from their structurally similar compounds [12,13]. Due to the advantages of selective separation of the sub-

* Corresponding authors. Tel.: +86 373 3325971; fax: +86 373 3326336.
E-mail address: fanjing@henannu.edu.cn (J. Fan).

0039-9140/$ – see front matter © 2011 Elsevier B.V. All rights reserved.
doi:10.1016/j.talanta.2011.03.015

strates, molecularly imprinted polymer (MIP) has been developed rapidly in samples pre-treatment, especially in the pre-treatment of environmental samples. Many conventional synthetic approaches toward imprinted polymer particles involve the synthesis of an imprinted polymer monolith [14]. The monolith then has to be ground and sieved to deliver a fraction of particles of desired size for the intended application. Particles prepared in this manner are typically irregular in shape and size, and the mass transfer is slow. In order to overcome these problems and improve the properties of MIP, different methods have been explored, including emulsion [15], precipitation [16,17], suspension and multistep swelling polymerization [18], film graft imprinting [19] and surface imprinting [20]. In these preparation methods, surface imprinting technique is welcome. The polymer with binding sites situated at the surface shows many advantages such as high selectivity, enhanced adsorption, more accessible sites, fast mass transfer and binding kinetics. In addition, it is known that the imprinted polymer materials synthesized by surface imprinting technology exhibit controllable size, regular shape, better mechanism intensity, and good reuse performance compared to the traditional imprinting materials. Thus, the surface molecularly imprinting technique has been the focus of more and more researches [21–25]. However, to the best of our knowledge, no molecularly imprinted polymer, especially surface imprinted polymer, has been reported for the separation and determination of alkyl-imidazolium based ionic liquids so far.

For the above reasons, we prepared, in this work, imidazole molecularly imprinted polymer by the surface imprinting technique using modified silica particles as the support material. It was found that there were effective imprinted sites on the surface of the imprinted polymer, and the polymer has been applied as solid-phase extraction material for the selective extraction of imidazole from its structural analogs. This work is expected to be the first step for the preparation of alkyl-imidazolium imprinted polymers.

2. Experimental

2.1. Materials and reagents

Silica particles (180–200 μm in diameter) and aminopropyltriethoxysilane were obtained from Qingdao Ocean Chemical Factory (Shandong, China) and Lancs Research Chemicals Ltd. (NJ, USA), respectively. Acryloyl chloride, methacrylic acid and ethylene dimethacrylate were purchased from Acros Company (NJ, USA). Imidazole, methanol, acetonitrile and chloroform were obtained from Tianjin Kermel Chemical Reagent Company (Tianjin, China). 1-Methylimidazole and the ionic liquids of 1-butyl-3-methylimidazolium chloride and 1-hexyl-3-methylimidazolium bromide were purchased from Henan Lihua Pharmaceutical Ltd. (Henan, China). Azobisisobutyronitrile, benzene, 2,4-dichlorophenol and m-dihydroxybenzene were from Beijing Chemical Reagent Company (Beijing, China). All these chemicals were of analytical reagent grade except for azobisisobutyronitrile which was of chemical purity grade. Methanol and acetonitrile of chromatographic purity were obtained from Zhengzhou Guoda Chemical Reagent Company (Henan, China). Ultra pure water was prepared from Milli-Q purification system (MilliPore, USA).

Azobisisobutyronitrile was recrystallized from methanol and then dried under reduced pressure before use. Methacrylic acid and ethylene dimethacrylate were distilled before use in order to remove the polymerization inhibitor. Chromatographic purity reagents were filtered through a 0.22 μm filter prior to use. Ultra pure water was used in the HPLC analysis and deionized water was used in other experiments.

2.2. Instruments

A T6 UV-vis spectrophotometer (Shanghai, China) and a high-performance liquid chromatography (Waters, USA) equipped with a reversed-phase column (C_{18} column, 4.6 mm × 150 mm), a C_{18} pre-column and a PDA 2998 ultraviolet–visible detector were used in the present work. Infrared spectra (IR) in KBr were recorded at 4000–400 cm^{-1} by using a Perkin-Elmer 983 infrared spectrophotometer (Norwalk, USA). The scanning electron microscope (SEM) micrographs of the sorbents were obtained at 20.0 kV on a JSM-5610LV scanning electron microscopy (JEOL, Japan). The ^1H NMR spectra were recorded by a AV-400 spectrometer (Bruker, Germany). The ASAP 2020 surface area and pore size analyzer (Micromeritics, USA) was used to measure the specific surface area, the total pore volume and the average pore diameters of the molecularly imprinting polymer and non-imprinted polymer.

2.3. Preparation of the imidazole imprinted polymer

A two-step procedure was used to prepare the imidazole imprinted polymer. The schematic expression for the synthetic route was illustrated in Fig. 1. In the first step, silica particles were modified chemically as described below. In order to increase the content of –OH, silica particles were activated by dipping into 6 mol L^{-1} hydrochloric acid for 24 h, then filtered and washed repeatedly with distilled water. Such treated silica particles were dried at 110 °C to constant weight. The activated silica particles were mixed with aminopropyltriethoxysilane (APTS) in anhydrous toluene in a sealed flask and then refluxed for 7 h. The resulting aminopropyltriethoxysilane–silica (APTS–silica) particles were separated, and washed with anhydrous toluene, ethanol and acetone in sequence. Then acryloyl chloride (AC) and the catalyst – triethylamine were mixed with aminopropyltriethoxysilane – modified silica particles in anhydrous toluene solution. The mixture was vigorously stirred for 12 h at room temperature under dry nitrogen. The product was separated by filtration and then washed successively with anhydrous toluene, methanol, ethanol and acetone. Finally, the obtained acryloyl chloride–aminopropyltriethoxysilane–silica (AC–APTS–silica) particles were dried under vacuum at 40 °C before use.

In the second step, imidazole imprinted polymer was prepared. For that purpose, 0.035 g of imidazole was dissolved in 50 mL of chloroform, and then 1.0 g of AC–APTS–silica particles and 0.18 mL of methacrylic acid (MAA) were added. The mixture was shaken at room temperature for 6 h for pre-polymerization. Then 1.89 mL of ethylene dimethacrylate (EDMA) and 0.010 g of azobisisobutyronitrile were added. The mixture was sonicated, and degassed with nitrogen for 10 min to eliminate oxygen, and then was sealed for polymerization at 60 °C for 24 h in a constant temperature incubating shaker with a rate of 200 rpm. The resultants were extracted with a mixed solvent of methanol/acetic acid (9:1, v/v) for 48 h in a Soxhlet extractor to remove the template. The obtained particles were washed with methanol till neutral and then dried to constant weight under vacuum at 60 °C. As a control, the non-imprinted polymer was prepared and treated under the same conditions except for the addition of the template.

2.4. Static adsorption tests

20.0 mg of the MIP and NIP particles were added, respectively, into 2.0 mL of acetonitrile in which imidazole or its structural analogs were contained. The mixtures were allowed to stand for 12 h at room temperature to facilitate the adsorption of imidazole or its analogs onto the MIP and NIP particles. After that, the concentration of the substrates in the supernatant solutions was

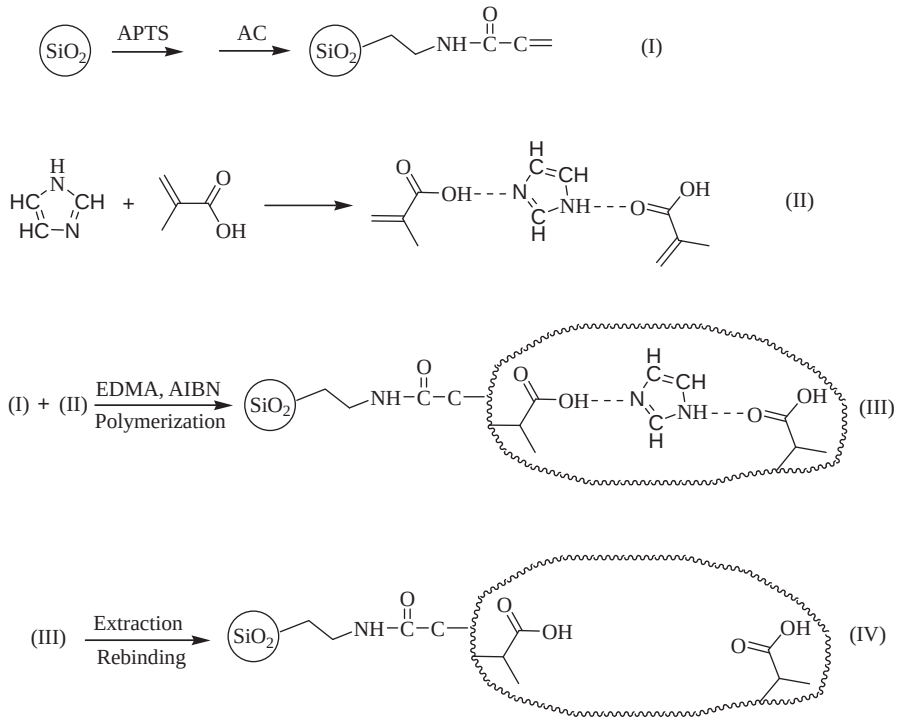

Fig. 1. Schematic illustration for the synthetic route of the molecularly imprinted polymer.

determined by a UV-vis spectrophotometer. The binding capacity of imidazole and the analogs was calculated from the equation:

$$Q = \frac{(C_0 - C)V1000}{M} \quad (1)$$

where Q stands for the binding capacity (μmol g^{-1}), C_0 and C are the initial and the residual concentrations (mmol L^{-1}) of imidazole or the analogs, respectively, V is the solution volume (mL), and M is the amount (mg) of the MIP or NIP particles used for the adsorption experiments.

2.5. Solid-phase extraction experiments

A homemade glass column (4.5 cm × 3 mm i.d.) packed with 100.0 mg of MIP was used as solid phase extraction (MIP–SPE) column, in which a small portion of glass wool was packed in order to prevent loss of the sorbent during sample loading. After the MIP–SPE column was pre-treated with methanol and acetonitrile, 1 mL of the sample solution containing 0.2 mmol L^{-1} imidazole or each of the structural analogs (1-methylimidazole, metronidazole or benzene) in acetonitrile was passed through the column at a flow rate of 0.5 mL min^{-1}. Then, the column was washed by methanol, and eluted by a mixed solvent of methanol/water (80:20, v/v). The eluate was analyzed by the HPLC. The NIP–SPE column was prepared and treated in the same way except that the stuffing was the NIP particles.

3. Results and discussion

3.1. Interaction between imidazole and the functional monomer

The principle of molecular imprinting lies in the preservation of the pre-polymerized host/guest structure into a polymer matrix. Thus it is important that the template and the functional monomer can form stable complexes through hydrogen bonding, ionic bonding or other interaction forces in the pre-polymerization mixture [26]. To understand the molecular recognition mechanism, the interaction between template and functional monomer should be studied.

Toward to this end, UV absorption spectra of the template (imidazole), functional monomer (methacrylic acid) and their mixture in acetonitrile were determined and the result was shown in Fig. 2. It can be seen that at the wavelength of 215 nm, the absorbance values of imidazole and methacrylic acid were 0.236 and 0.844, respectively. However, the absorbance of their mixture was 0.891, which was much lower than the summation of 0.236 and 0.844. This difference was resulted from the interactions of imidazole with methacrylic acid. Due to the pre-polymerization, the complex of imidazole with methacrylic acid was formed probably through hydrogen bonding and/or ionic bonding between N–H of imidazole and –COOH of methacrylic acid.

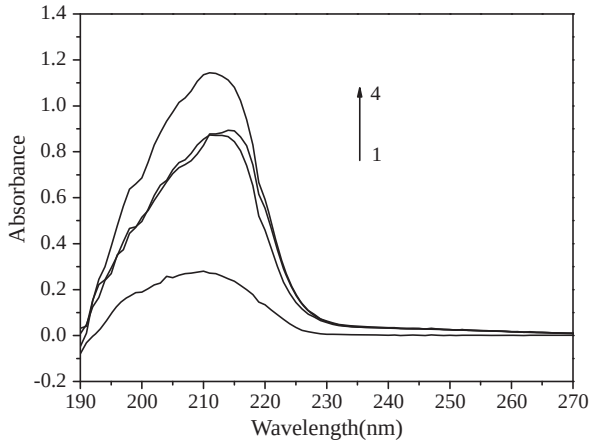

Fig. 2. UV absorption spectra of imidazole in the presence of methacrylic acid in acetonitrile: (1) imidazole (0.125 mmol L^{-1}); (2) methacrylic acid (0.5 mmol L^{-1}); (3) the mixture of 1 and 2; (4) the sum of adsorption values for 1 and 2.

Table 1
Some structural parameters for MIP and NIP.

	Specific surface area[a] ($m^2\ g^{-1}$)	Total pore volume[b] ($cm^3\ g^{-1}$)	Average pore diameter[b] (nm)
MIP	206.04	0.29	5.22
NIP	230.54	0.39	5.74

[a] Measured by Brunauer–Emmett–Teller (BET) method.
[b] Measured by Barrett–Joyner–Halenda (BJH) method.

A comparison of ^{1}H NMR spectra for imidazole, methacrylic acid and their mixture was shown in Fig. 3. The proton of N-1 and the proton of C-2 on the imidazole ring shifted downfield from 12.101 and 7.646 ppm (spectrum a) to 12.797 and 8.025 ppm (spectrum c), respectively, in the presence of methacrylic acid. Meanwhile, the downfield chemical shift of proton of the carboxyl group was from 12.388 ppm (spectrum b) to 12.797 ppm (spectrum c) due to the interaction between imidazole and methacrlic acid. All these data suggested the formation of hydrogen bonding and/or ionic bonding between imidazole and methacrylic acid.

3.2. Characteristics of MIP and NIP

The morphology of MIP and NIP observed from SEM was shown in Fig. 4. It was found that shape of the polymers was uniform, and the size was close to that of the silica particles. The possible reason was that the polymerization reaction occurred on the surface of silica particles, and the coating was very thin so that the shape and size of silica particles and the polymers were very similar. It was also found from the magnified SEM photos (not shown) that the micro-pore on the surface of NIP was well-distributed but the average pore diameter was smaller than that of MIP. This may be ascribed to the elution of template molecules in the preparation of MIP. Table 1 lists the results of nitrogen adsorption experiments for MIP and NIP particles. It can be seen that the specific surface area, the total pore volume and the average pore diameter were different for MIP and NIP particles. These data support the observation from SEM photos.

Fig. 5 shows IR spectra of the silica gel-based samples. Obviously, APTS–silica displayed the characteristic peaks of amino groups at 1538 cm^{-1}, while AC–APTS–silica exhibited the relatively strong band of carbonyl group at 1665 cm^{-1}. This observation reveals that the two-step chemical modification was achieved at the surface of silica particles. In addition, the band at around 2959 cm^{-1} was assigned to the stretching vibration of $-CH_2-$ or $-CH_3$, the band at 1732 cm^{-1} was assigned to the absorption of –COOH, and the bands at 1233 and 1105 cm^{-1} were ascribed to the stretching vibrations of C–O–C. The absorption peaks of MIP and NIP particles were similar, which means that no template molecules were retained on the MIP.

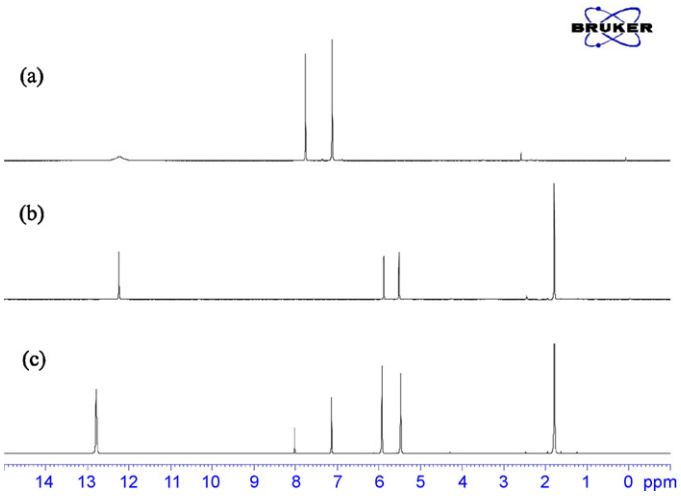

Fig. 3. ^{1}H NMR spectra of imidazole, methacrylic acid and their mixture in DMSO: (a) imidazole (0.15 mol L^{-1}); (b) methacrylic acid (0.60 mol L^{-1}); (c) imidazole (0.15 mol L^{-1}) + methacrylic acid (0.60 mol L^{-1}).

3.3. Molar ratio optimization of the template and the functional monomer

Although the binding capacity is an effective parameter for the performance evaluation of the molecularly imprinted polymer, the ability of selective adsorption is more important for their application. Therefore, it would be very significant to investigate the ability of selective recognition of the molecularly imprinted polymer for the template molecules. For this purpose, three different molar ratios of imidazole to methacrylic acid were studied in the preparation of MIP and NIP. The binding capacity (μmol g^{-1}) of imidazole on these polymers was determined and used to calculate the imprinting factor [23] from the equation:

$$\beta = \frac{Q_{MIP}}{Q_{NIP}} \quad (2)$$

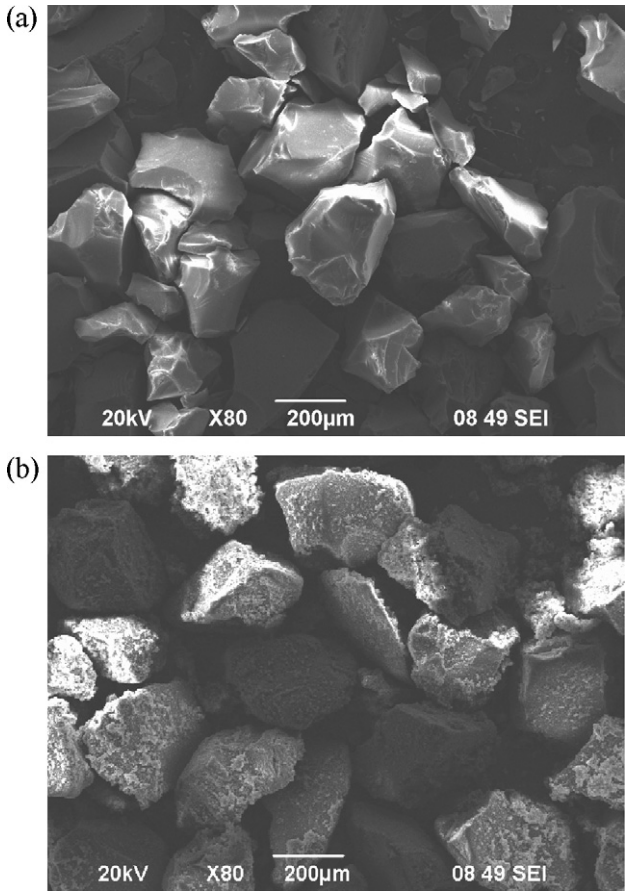

Fig. 4. SEM micrographs: (a) silica particle; (b) MIP.

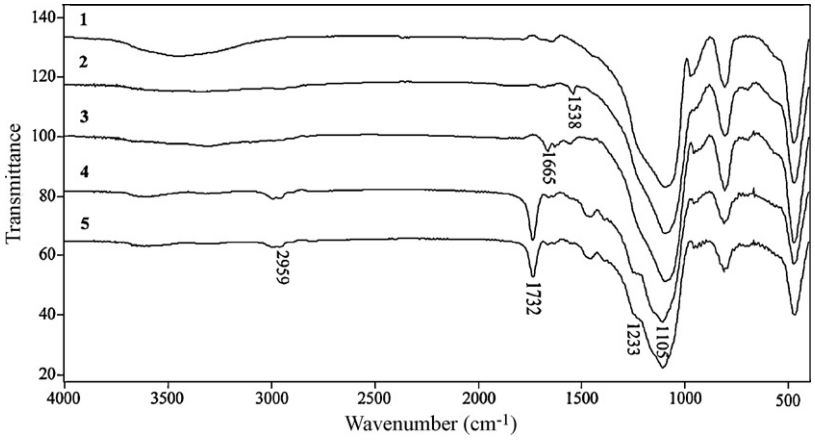

Fig. 5. IR spectra of silica gel-based samples: (1) pure silica; (2) APTS–silica; (3) AC–APTS–silica; (4) MIP; (5) NIP.

Here, β is the imprinting factor of the MIP, Q_{MIP} and Q_{NIP} stand for the binding capacity of imidazole on the MIP and NIP material. The results were given in Table 2. It can be seen that among the three molar ratios of imidazole to methacrylic acid, the binding capacity of the polymers prepared at the ratio of 1:6 was maximum, whereas that at the ratio of 1:2 was minimum. The possible reason was that the non-specific binding sites increased with increasing proportion of methacrylic acid, which resulted in the increase of the bound amount of imidazole. However, the imprinting factor (2.29) of the polymers prepared at the ratio of 1:4 was the highest. This suggests that the complex of imidazole with methacrylic acid was optimal, and the ability of the polymer for selective adsorption of imidazole was the strongest at this molar ratio. Therefore, 1:4 of imidazole to methacrylic acid was chosen as the right molar ratio for the preparation of MIP.

3.4. Binding isotherms of imidazole on the MIP and NIP

The binding isotherm curves of imidazole on the MIP and NIP were plotted in Fig. 6. It was shown that the binding capacity of the polymers increased with increasing initial concentration of imidazole in the range of 1.0–10.0 mmol L^{-1}, and the MIP had higher affinity for imidazole than NIP. In the higher concentration range, the binding capacity was close to be stable. The binding data can be analyzed by Langmuir equation:

$$Q = \frac{Q_{max} C_{eq}}{B + C_{eq}} \quad (3)$$

where Q stands for the binding capacity (μmol g^{-1}), Q_{max} is the maximum binding capacity (μmol g^{-1}), C_{eq} is equilibrium concentration of imidazole (mmol L^{-1}), and B is a constant. In order to calculate the maximum binding capacity of imidazole on both MIP and NIP, this equation was changed into Eq. (4):

$$\frac{C_{eq}}{Q} = \frac{C_{eq}}{Q_{max}} + \frac{B}{Q_{max}} \quad (4)$$

Actually, Eq. (4) shows a linear relationship between C_{eq}/Q and C_{eq}. From the slope of the linear plot, the maximum binding capacity of imidazole on the MIP and NIP was calculated to be 312 and 169 μmol g^{-1}, respectively, indicating that the maximum binding capacity of imidazole on MIP was 1.84 times of that on NIP. This difference suggested that the spatial structure of MIP and NIP materials was different though their chemical composition was similar. There existed cavities and specific rebinding sites for imidazole on the MIP because the structure of template–monomer complex, which is possibly resulted from the ionic bonding or hydrogen bonding between –NH and –CH (2-position) in the imidazole molecules and –COOH in the function monomer, was in accordance with the shape and structure of template molecules. However, there were no these "memory" sites in NIP, so that its binding capacity was lower. Therefore, it is very important to form cavities and specific rebinding sites for the recognition of the template molecules.

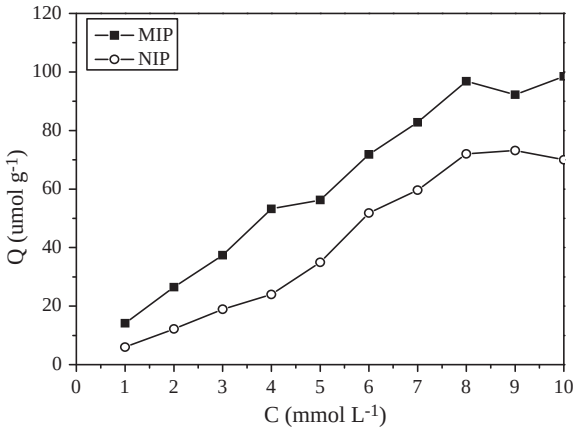

Fig. 6. Adsorption isotherms of imidazole on MIP and NIP.

In general, the large pore volume results in the large specific surface area, this is advantageous for the polymer to adsorb the template molecules [27]. It was found from Table 1 that the specific surface area and average pore volume of NIP were larger than those of MIP, but the binding capacity of NIP was smaller than that of MIP. This indicates that MIP has strong specific adsorption for imidazole.

3.5. Binding kinetic curve of imidazole on the MIP

In Fig. 7, the adsorption kinetic curve of imidazole on MIP was shown at the imidazole concentration of 3.0 mmol L^{-1} in acetonitrile. It can be seen that the binding capacity increased rapidly in initial 30 min, and then turned to a plateau. Because MIP was poly-

Table 2
Binding capacity and imprinting factor for the molecularly imprinted polymers prepared at different molar ratios of template to functional monomer.

n_i/n_m [a]	Q_{MIP} (μmol g^{-1})	Q_{NIP} (μmol g^{-1})	β
1:2	13.0	7.5	1.73
1:4	20.0	8.7	2.29
1:6	36.0	28.5	1.26

[a] n_i and n_m are the molar number of imidazole and methacrylic acid, respectively.

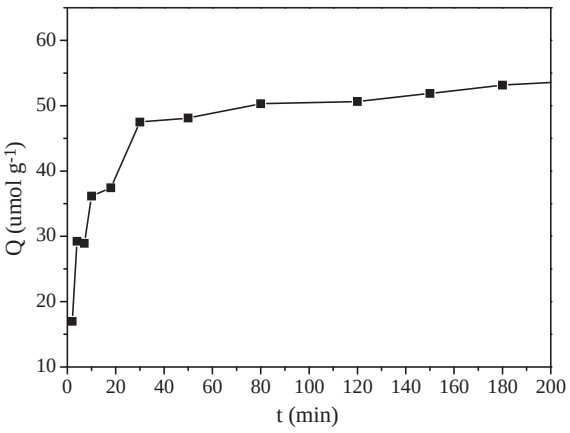

Fig. 7. Adsorption kinetic curve of imidazole on MIP.

merized on the surface of silica particles, a thin layer of imprinted material containing recognition sites was only on the surface. The template can be extracted completely following the creation of the imprint sites during the imprinting step. Also, the template molecules can reach the imprint sites easily and quickly during the rebinding step [28]. Therefore, MIP showed good site accessibility for imidazole and the equilibrium was achieved quickly. However, in the MIP synthesized by bulk polymerization, the recognition sites were not only on the surface but also in the inside of cross linked polymer network, and the mass transfer of the obtained monolith polymer was slow so that the adsorption equilibrium would be achieved in a long period of time. These features are not well-suited for the analysis of real samples. The imprinted polymer synthesized by surface imprinting technique overcame these drawbacks.

For solid/solution systems, the pseudo-first order kinetic model (5) or the pseudo-second order kinetic model (6):

$$\ln(Q_e - Q_t) = \ln \quad Q_e - k_a t \tag{5}$$

$$\frac{t}{Q_t} = \frac{t}{Q_e} + \frac{1}{k_b {Q_e}^2} \tag{6}$$

can be used to describe the binding process [29]. In these equations, K_a and K_b are the rate constants for the first order sorption and the second order sorption processes, respectively. Q_t stands for the binding capacity (μmol g^{-1}) at given time t, and Q_e indicates the equilibrium binding capacity (μmol g^{-1}). The pseudo-first order kinetic model is the most widely used rate equation to describe the adsorption of a solute from liquid solution. However, when the pseudo-first order kinetic model was applied to the experiment data, no linear relationship was observed, and this model has been found to be unsatisfactory in providing a concrete mechanism for the adsorption process in an equally good number of cases [30,31]. In the pseudo-second order model, the chemisorption of the adsorbate on the adsorbent was considered to be the rate-limiting step, and the solute molecules reacted with two kinds of adsorption sites. If the pseudo-second order model was used to treat the experimental data, t/Q_t versus t yielded a linear plot ($y = 0.10899 + 0.01829\,x$) with correlation coefficient of 0.9996. This suggests that the binding process can be described by the pseudo-second order model, and chemisorption is the rate-controlling step [31]. It is the two different types of functional groups of imidazole molecule which formed two kinds of complexes with methacrylic acid, leading to two kinds of binding sites for MIP in molecular recognition process.

3.6. Selective adsorption

Selective adsorption experiments were carried out in acetonitrile solution containing 3.0 mmol L^{-1} imidazole or a series of structural analogs 1-methylimidazole, benzene, 2,4-dichlorophenol, m-dihydroxybenzene, 1-butyl-3-methylimidazolium chloride ([C$_4$mim][Cl]) and 1-hexyl-3-methylimidazolium bromide ([C$_6$mim][Br]) (their molecular structures are shown in Fig. 8), and the binding capacity of these compounds on the MIP and NIP was investigated by the equilibrium binding approaches. Here we use ΔQ ($\Delta Q = Q_{MIP} - Q_{NIP}$) as the parameter for the evaluation of selective adsorption of the polymer [32]. From the results listed in Table 3, it is obvious that the binding capacity of imidazole and 1-methylimidazole on the MIP was much higher than that on the NIP, and the ΔQ value was the maximum for imidazole except for benzene. This result suggested that the complexes between –NH and –CH (2-position) in the imidazole molecules and –COOH in the function monomer were formed by ionic bonding or hydrogen bonding. In the procedure of elution, the template molecule was washed out, and the cavities matched with the template molecules in shape and size were then created, which recognized the template molecules effectively. Although the chemical composition of MIP and NIP is the same, the latter polymer can only bind the tested compounds by non-specific adsorption due to the absence of proper cavities and recognition sites in this polymer. 1-Methylimidazole has similar size and structure with imidazole, which led to the higher binding capacity than the other structural analogs. However, the size of 1-butyl-3-methylimidazolium ([C$_4$mim][Cl]), 1-hexyl-3-methylimidazolium ([C$_6$mim][Br]) and benzene derivatives was much larger than that of imidazole though there were –CH (2-position) in [C$_4$mim][Cl] and [C$_6$mim][Br]. Therefore, their binding capacity was smaller than that of imidazole.

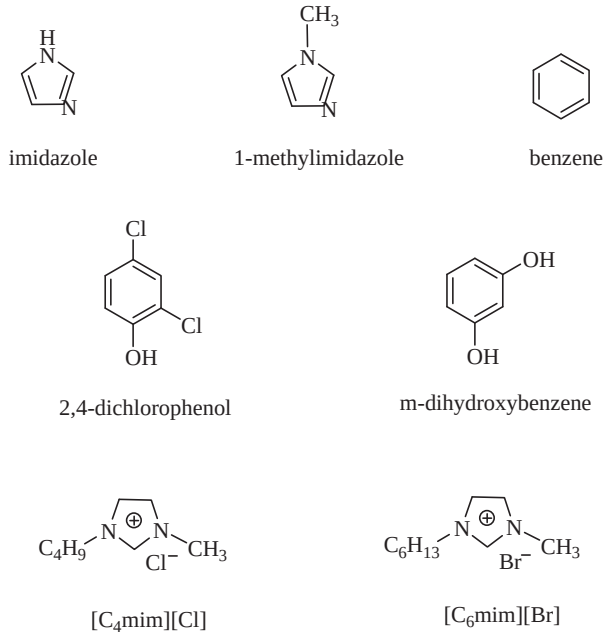

Fig. 8. Structures of imidazole and its analogs.

Table 3
Binding capacity of different substrates on MIP and NIP.

Substrates	Q_{MIP} (μmol g^{-1})	Q_{NIP} (μmol g^{-1})	ΔQ (μmol g^{-1})
Imidazole	46.46	21.71	24.75
1-Methylimidazole	17.73	2.53	15.2
Benzene	225.35	72.90	152.45
2,4-Dichlorophenol	0.52	0.00	0.52
m-Dihydroxybenzen	4.21	2.16	2.05
[C$_4$mim][Cl]	3.96	1.89	2.07
[C$_6$mim][Br]	5.05	2.83	2.22

Table 4
Recoveries of imidazole (IM), 1-methylimidazole (1-ME), metronidazole (MET), and benzene (BEN) from MIP and NIP columns.[a]

	MIP				NIP			
	IM	1-ME	MET	BEN	IM	1-ME	MET	BEN
Effluent (%)	0	10	72.3	22.5	27.5	75	98.4	45
First wash (%)	15.0	65.0	8.7	70.0	5.0	0	2.9	0
Second wash (%)	0	0	0	0	30.0	0	0	60.0
Third wash (%)	0	0	0	0	35.0	0	0	0
Elution (%)	87.5	17.5	19.3	10.0	0	32.5	3.8	5.0
Total recovery (%)	102.5	92.5	100.3	102.5	97.5	107.5	105.1	110

[a] For each washing and elution, 5 mL of methanol and 5 mL of methanol/water (80:20, v/v) were used, respectively.

On the other hand, results in Table 3 indicate that the binding capacity increases with decreasing polarity of the compounds. For example, the polarity of benzene is the lowest among the structural analogs, but its binding capacity is the highest. This suggests that in the recognition of benzene, the non-specific binding was the main binding mode. From these results, it can be concluded that both the size of the target compounds and the non-covalent interactions were very important in the binding process.

3.7. Solid-phase adsorption behavior of the polymers

3.7.1. Effect of flow rate and desorption solvent

In the solid-phase extraction column experiment, flow rate of solution and eluent was an important parameter affecting the binding of IM. In order to optimize this factor, the influence of flow rate on IM binding was studied in the range from 0.2 to 2.0 mL min^{-1} and desorption solvent were examined by a batch mode experiment. For this purpose, 100.0 mg of MIP was mixed with methanol and packed in a glass column, and 5 mL of acetonitrile solution containing 10 μg IM was allowed to pass through the column. It was shown that about 100% of IM was bound by MIP when the flow rate was less than 1.2 mL min^{-1}, but the retention of IM was only 92.8% when the flow rate was up to 1.6 mL min^{-1}. It is well known that when the flow rate is too fast, IM cannot sufficiently be adsorbed by MIP in the column. Therefore, we choose 0.5 mL min^{-1} as the best flow rate in our experiment. Then IM retained in the column was eluted by methanol, acetonitrile and a mixed solvent of methanol/water, respectively. The result suggests that the mixed solvent of methanol/water (80:20, v/v) was the best desorption solvent.

3.7.2. Selectivity of the MIP–SPE and NIP–SPE columns

Here, imidazole, imidazole-derivatives (1-methylimidazole and metronidazole) and benzene were chosen to study the selective adsorption behavior of the MIP–SPE and NIP–SPE columns. After loading of sample solutions, the remained concentrations of the compounds in effluents and eluents from the MIP–SPE and NIP–SPE columns were determined, respectively. The adsorption and recovery results were given in Table 4. It can be seen that the binding capacities of the samples on MIP–SPE column were much higher than that on NIP–SPE column, and that imidazole could be retained completely on the MIP–SPE column, while 1-methylimidazole, metronidazole and benzene could be retained only in different extents on both of the columns. After three times washing, most of the imidazole-derivatives and benzene could be washed off from the columns, but more than 87% of imidazole was still bound on the MIP–SPE column. This indicates that the MIP material has excellent molecular recognition ability and high selectivity for imidazole. In contrast, the NIP material has no this ability, and the interaction between targets and the polymer was non-specific affinity. In addition, it was observed that benzene could be washed off from the SPE columns easily after two times washing. This illustrated again that the highest binding amount of benzene shown in Table 3 was resulted from its non-specific affinity to the polymers. Considering the fact that among the test compounds, the polarity of benzene is low and its interaction with the solvent (acetonitrile) is weak, benzene would be apt to bind with the sorbent by the non-selective adsorption during the equilibrium binding process. These results suggest that it is possible to selectively enrich and separate imidazole from its structural analogs by using the MIP material.

3.8. HPLC evaluation of the selective separation

In order to further investigated whether the MIP–SPE column can be used for the selective separation and enrichment of imidazole from a mixture of its structural analogs, chromatographic experiment was carried out by passing 5.0 mL of acetonitrile solution, containing 2.0 mg L^{-1} imidazole, 2.0 mg L^{-1} 1-hexyl-3-methylimidazolium bromide ([C_6mim][Br]) and 2.0 mg L^{-1} 2,4-dichlorophenol, through the column at a flow rate of 0.5 mL·min^{-1}, where [C_6mim][Br] and 2,4-dichlorophenol were used as interference species. Then the column was eluted with 1 mL of methanol–water solution (80:20, v/v), and the analyte in the eluate was analyzed by the HPLC with a flow rate of 0.5 mL min^{-1} at 30 °C. The mobile phase used for HPLC experiment was a mixture of methanol and water (80:20, v/v), and the UV–vis detector was operated at 215 nm. The chromatograms for the mixed solution of imidazole, 1-hexyl-3-methylimidazolium bromide ([C_6mim][Br]) and 2,4-dichlorophenol in acetonitrile with and without solid-phase extraction treatment by MIP were shown in Fig. 9. In this figure, peaks 1, 2 and 3 were identified as ([C_6mim][Br]), imidazole and 2,4-dichlorophenol, respectively. Compared with the signals shown in Fig. 9a, it could be found from Fig. 9b that imidazole could be bound well, but [C_6mim][Br] and 2,4-dichlorophenol were bound poorly on the MIP–SPE column. After elution from MIP–SPE column, the recovery is 97.6–102.7% for imidazole and 12.2–17.3% for [C_6mim][Br], but 2,4-dichlorophenol in the eluate could not be determined by HPLC under the experimental conditions. Therefore, it is appropriate to state that MIP would be used as a solid-phase sorbent to separate and enrich imidazole from complex matrix.

One of the advantages of MIP–SPE sorbents is their reusability. In order to test this performance of the MIP–SPE column, the mixed solution containing imidazole, [C_6mim][Br] and 2,4-dichlorophenol in acetonitrile was passed through the MIP–SPE column at the rate of 0.5 mL min^{-1}, and the concentration of imidazole in the mixture was kept at 0.2 mmol L^{-1}. After elution by a mixed solvent of methanol–water (80:20, v/v), the eluate was analyzed by HPLC. The result showed that the recovery of imidazole was higher than 94%, and no significant decrease in selectivity had been observed after fifty times of reuse of the MIP–SPE column.

3.9. Application to environmental water samples

To demonstrate the ability of MIP to extract IM from real samples, the trace of IM in lake water, ground water and tap water were determined under the optimized conditions by coupling MIP–SPE

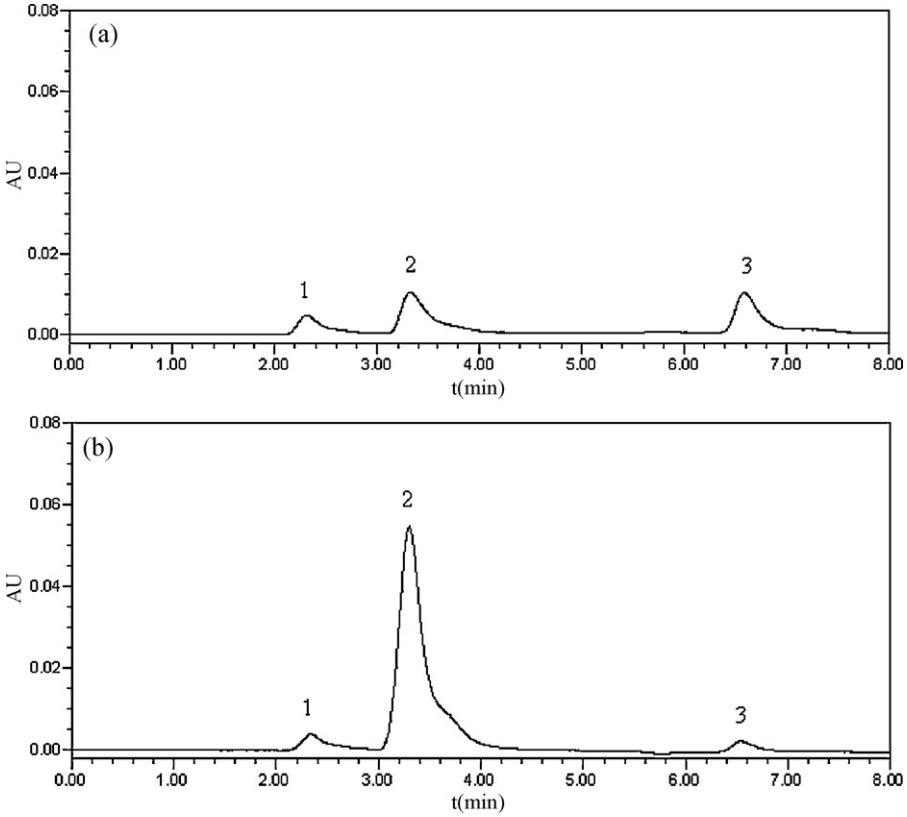

Fig. 9. Chromatograms for a mixture of imidazole, [C_6mim][Br] and 2,4-dichlorophenol: (a) mixture without extraction by the MIP–SPE column; (b) eluate of the mixture from the MIP–SPE column. Chromatographic conditions of C_{18} reversed-phase column: detection wavelength, 215 nm; mobile phase, methanol–water (80:20, v/v); flow rate, 0.5 mL min^{-1}; column temperature, 30 °C.

Table 5
Determination of imidazole after MIP–SPE column in real water samples (n = 3).

Samples	Add (mg L^{-1})	Detected (mg L^{-1})	Recovery (%)	R.S.D. (%)
Lake water	–	–	–	–
Lake water	0.30	0.29	96.7	4.3
Lake water	1.00	0.99	99.0	3.6
Ground water	–	–	–	–
Ground water	0.30	0.29	96.7	3.3
Ground water	1.00	0.94	94.0	2.9
Tap water	–	–	–	–
Tap water	0.30	0.30	100.0	5.3
Tap water	1.00	1.00	100.0	1.0

and HPLC. In the practical water samples, the lake water was sampled from Muye Lake in Xinxiang, the tap water was taken from our laboratory, and the ground water from Xinxiang City. The water samples were filtered to eliminate the solid impurity, and a suitable amount of water sample was passed through the MIP–SPE column. The eluent was collected and the content of IM in the eluent was determined. It can be seen from Table 5 that no IM was detected in the samples of lake water, ground water and tap water. When 0.3 and 1.0 mg L^{-1} of IM were added, the recoveries of IM were found to be in the range from 94.0 to 100.0% for the three water samples. These results confirmed that the MIP prepared in the present work could be effectively applied for the determination of IM in real samples.

4. Conclusions

In this work, we prepared a new molecularly imprinted polymer by surface polymerization with imidazole as the template and silica particles as the support matrix. The structural and adsorption characteristics of this polymer have been studied. From our experimental results, the following conclusions have been drawn: (i) the shape and size of the molecularly imprinted polymer were similar to that of the silica particles, and the imprinting factor was the highest for the imprinted polymer prepared at the molar ratio of 1:4 of the template to the functional monomer; (ii) the MIP has strong ability of selective recognition and specific adsorption for imidazole, and can be used as an excellent solid-phase sorbent to separate and enrich imidazole from its structural analogs, suggesting that the cavities and specific rebinding sites on the surface of the imprinted polymer play an important role in the recognition process of substrates; (iii) the adsorption was fast and the adsorption equilibrium was achieved in 30 min, and the binding process could be described by pseudo-second order kinetics; (iv) the polymer can be reused without significant decrease in selectivity. To the best of our knowledge, this is the first report on the molecularly imprinted polymer for the separation and enrichment of imidazole. The information obtained here is important for the solid phase extraction and determination of trace imidazole

in environmental water samples. Also, this may lay the basis for the preparation of alkyl-imidazolium imprinted polymers used for the separation and determination of alkyl-imidazolium based ionic liquids.

Acknowledgments

This work was supported financially by the National Natural Science Foundation of China (Grant no. 20977025) and the Doctoral Foundation of Ministry of Education of China (Grant no. 200804760004).

References

[1] Y.C. Pei, J.J. Wang, X.P. Xuan, J. Fan, M.H. Fan, Environ. Sci. Technol. 41 (2007) 5090–5095.
[2] X.W. Chen, Y.P. Ji, J.H. Wang, Analyst 135 (2010) 2241–2248.
[3] J. Ranke, K. Molter, F. Stock, U. Bottin-Weber, J. Poczobutt, J. Hoffmann, B. Ondruschka, J. Filser, B. Jastorffa, Ecotoxicol. Environ. Saf. 58 (2004) 396–404.
[4] P. Stepnowski, A.C. Skladanowski, A. Ludwiczak, E. Laczynska, Hum. Exp. Toxicol. 23 (2004) 513–517.
[5] D.J. Couling, R.J. Bernot, K.M. Docherty, J.K. Dixon, E.J. Maginn, Green Chem. 8 (2006) 82–90.
[6] M. Matsumoto, K. Mochiduki, K. Kondo, J. Biosci. Bioeng. 98 (2004) 344–347.
[7] C.W. Cho, Y.C. Jeon, T.P.T. Pham, K. Vijayaraghavan, Y.S. Yun, Ecotoxicol. Environ. Saf. 71 (2008) 166–171.
[8] N. Zhang, C. Lu, J.G. Li, Q.Q. Li, Talanta 81 (2010) 698–702.
[9] I. Billard, G. Moutiers, A. Labet, A.E. Azzi, C. Gaillard, C. Mariet, K. Lutzenkirchen, Inorg. Chem. 42 (2003) 1726–1733.
[10] X.H. Li, H.L. Duan, J.T. Pan, Chin. J. Anal. Chem. 34 (2006) 192–194.
[11] J.S. Torrecilla, E. Rojo, J. Garca, F. Rodrguez, Ind. Eng. Chem. Res. 47 (2008) 4025–4028.
[12] M. Javanbakht, M.H. Namjumanesh, B. Akbari-adergani, Talanta 80 (2009) 133–138.
[13] X.W. Kan, Q. Zhao, Z. Zhang, Z.L. Wang, J.J. Zhu, Talanta 75 (2008) 22–26.
[14] A. Beltran, R.M. Marce, P.A.G. Cormack, F. Borrull, J. Chromatogr. A 1216 (2009) 2248–2253.
[15] S.R. Carter, S. Rimmer, Adv. Funct. Mater. 14 (2004) 553–561.
[16] L. Ye, I. Surugiu, K. Haupt, Anal. Chem. 74 (2002) 959–964.
[17] N. Sai, Y.P. Chen, N. Liu, G.G. Yu, P. Su, Y. Feng, Z.J. Zhou, X.Y. Liu, H.Y. Zhou, Z.X. Gao, B.A. Ning, Talanta 82 (2010) 1113–1121.
[18] Y. Watabe, T. Kubo, T. Nishikawa, T. Fujita, K. Kaya, K. Hosoya, J. Chromatogr. A 1120 (2006) 252–259.
[19] T. Piacham, A. Josell, H. Arwin, V. Prachayasittikul, L. Ye, Anal. Chim. Acta 536 (2005) 191–196.
[20] W. Luo, L.H. Zhu, C. Yu, H.Q. Tang, H.X. Yu, X. Li, X. Zhang, Anal. Chim. Acta 618 (2008) 147–156.
[21] R.Z. Ouyang, J.P. Lei, H.X. Ju, Chem. Commun. (2008) 5761–5763.
[22] L. Qin, X.W. He, W. Zhang, W.Y. Li, Y.K. Zhang, J. Chromatogr. A 1216 (2009) 807–814.
[23] H.M. Liu, C.H. Liu, X.J. Yang, S.J. Zeng, Y.Q. Xiong, W.J. Xu, Anal. Chim. Acta 628 (2008) 87–94.
[24] C. Tan, S. Wangrangsimakul, R. Bai, Y.W. Tong, Chem. Mater. 20 (2008) 118–127.
[25] D.M. Gao, Z.P. Zhang, M.H. Wu, C.G. Xie, G.J. Guan, D.P. Wang, J. Am. Chem. Soc. 129 (2007) 7859–7866.
[26] J. Fan, Y.F. Wei, J.J. Wang, C.L. Wu, H.L. Shi, Anal. Chim. Acta 639 (2009) 42–50.
[27] S.G. Hu, L. Li, X.W. He, Anal. Chim. Acta 639 (2009) 42–50.
[28] C.H. Lu, W.H. Zhou, B. Han, H.H. Yang, X. Chen, X.R. Wang, Anal. Chem. 79 (2007) 5457–5461.
[29] W. Rudzinski, W. Plazinski, J. Phys. Chem. B 110 (2006) 16514–16525.
[30] Y.S. Hoa, G. McKay, Fellow Trans. Icheme E 76B (1998) 332–340.
[31] Y.S. Hoa, G. McKay, Fellow Trans. Icheme E 77B (1999) 165–173.
[32] X. Feas, J.A. Seijas, M.P. Vazquez-Tato, P. Regal, A. Cepeda, C. Fente, Anal. Chim. Acta 631 (2009) 237–244.